Transactions of the VŠB – Technical University of Ostrava, Mechanical Series
No. 3, 2009, vol. LV
article No. 1722

Pavel GEJDOŠ[*], Josef ZAPLETAL[**], Tomáš PODRÁBSKÝ[***]

FATIGUE PROPERTIES OF AZ31 MAGNESIUM ALLOY WITH CALCIUM ADDITION

ÚNAVOVÉ VLASTNOSTI HOŘČÍKOVÉ SLITINY AZ31 S PŘIDANÝM VÁPNÍKEM

Abstract

In the work the AZ31 magnesium alloy with 0.15% calcium was studied which was cast using squeeze casting (SC). Besides the determination of mechanical and fatigue properties also microstructure of the alloy was observed. In addition, fractographic evaluation of the resulting fracture surfaces after fatigue loading was performed.

Abstrakt

V práci byly zjištěny mechanické a únavové vlastnosti hořčíkové slitiny AZ31 s 0,15 % vápníku, která byla odlita metodou squeeze casting (SC). Také bylo provedeno pozorování mikrostruktury dané slitiny. Na vzniklých lomových plochách po únavovém zatěžování bylo provedeno fraktografické zhodnocení lomových ploch.

1 INTRODUCTION

Low density is mostly the reason why the magnesium alloys find more and more applications, nowadays. Degreasing the mass of e.g. a car means decreasing its gasoline consumption which represents favourable consequences from economic and ecologic point of view. This can be also the reason for wider and wider applications of magnesium alloys in aerospace and automotive industry. Besides of that, the resulting low weight of the final products is important for consumers of electronics and sport articles, therefore, the application of magnesium alloys extends across these branches.

To improve the properties of magnesium alloys, several alloying elements are added. One of them is calcium, added in order to decrease grain size or to limit the combustibility during casting [1]. The calcium added can impact also other properties.

2 EXPERIMENTAL MATERIAL

As experimental material the AZ31 magnesium alloy with added 0.15 % Ca, which was cast using the squeeze casting was used in this work. Its chemical composition was determined using Spectrumat GDS 750 optical emission spectrometer with glow discharge. To asses the calcium content, the Thermo Solaar M6 absorption atomic spectrometer was used. The results of measurements of both the methods together with the values from the ASTM standard (AZ31B) are shown in Table 1 where the values represent the average of 3 measurements. Magnesium content is the rest up to 100 %.

[*] Ing. Pavel Gejdoš, Institute of Materials Science and Engineering, Faculty of Mechanical Engineering, Brno University of Technology, Technická 2, Brno, tel. (+420) 54 114 3466, e-mail gejdos@fme.vutbr.cz

[**] Ing. Josef Zapletal, Institute of Materials Science and Engineering, Faculty of Mechanical Engineering, Brno University of Technology, Technická 2, Brno, tel. (+420) 54 114 3466, e-mail pepa.sanguis@centrum.cz

[***] Prof. Ing. Tomáš Podrábský, CSc., Institute of Material Science and Engineering, Faculty of Mechanical Engineering, Brno University of Technology, Technická 2, Brno, tel. (+420) 54 114 3150, e-mail podrabsky@fme.vutbr.cz

Tab. 1 Chemical composition of magnesium alloy AZ31 SC (in wt.%).

Element	Al	Zn	Cu	Mn	Si	Fe	Ni	Ca
ASTM	2.5÷3.5	0.6÷1.4	max. 0.04	0.20÷1.0	max. 0.10	max. 0.005	max. 0.005	–
Measured	2.51	0.94	0.00	~ 0.45	0.00	0.004	0.00	0.141

3 RESULTS AND DISCUSSION

3.1 The metallographic evaluation of the structure

The samples were prepared in normal way using Struers LaboPress-3 press. Metallographic structure was etched using acetic picric mixture composed of 5 ml acetic acid, 6 g picric acid, 10 ml water and 100 ml ethanol [2]. The Olympus GX71 light microscope with Olympus DP11 digital camera was used to observe the surface of etched cuts.

Metallographic cuts were also exploited for local analysis of chemical composition of appearing phases using the Philips XL 30 scanning electron microscope with energy dispersive spectrometer EDAX. According to the results of this analysis and comparing them with literature [1, 3, 4], the matrix of the alloy consists of magnesium and a small quantity of aluminium (1.45 wt.%). The point analysis of the chemical composition gives also that the calcium added is found only along grain boundaries where it creates $(Mg, Al)_2Ca$ phase. Fig. 1 shows the structure of the alloy using SEM, Fig. 2 using light microscope. In both figures identified phases are marked.

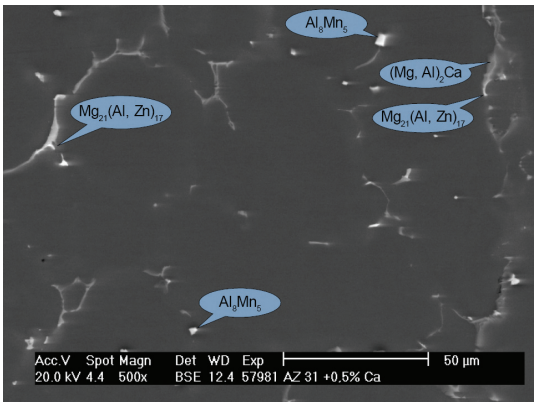

Fig. 1 AZ31 SC + 0.15% Ca, picric acid, SEM.

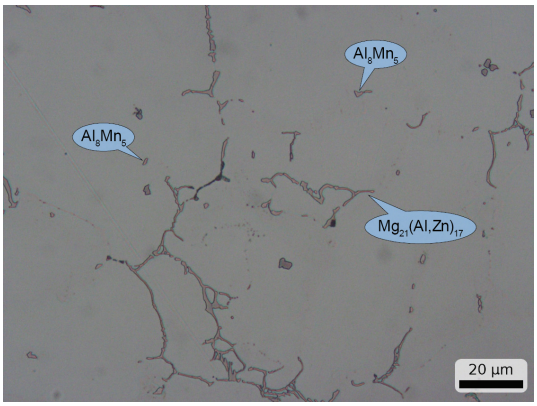

Fig. 2 AZ31 SC + 0.15% Ca, picric acid, LM

3.2 Determination of mechanical properties

The tensile tests of cylindrical test bars with threaded heads (diameter $d_0 = 6$ mm, measured length $L_0 = 30$ mm) were performed using a computer controlled test machine. The averages and standard deviations of 4 measurements are shown in Table 2.

Tab. 2 Mechanical properties.

	$R_{p0,2}$ [MPa]	R_m [MPa]	A [%]	Z [%]
Average	76	193	10.6	9.7
Standard deviation	1	8	1.3	2.4

With regard to the fact that the material is cast, its strength and plastic properties are relatively good in comparison with extruded or rolled material [5, 6, 7], only its yield strength $R_{p0,2}$ is lower.

3.3 Experimental determination of fatigue properties

Fatigue tests of cylindrical test bars with threaded heads with diameter $d_0 = 6$ mm were performed using the Instron 8801 servo-hydraulic machine in the mode of force control. The specimens were loaded at symmetric tensile-compression load cycles ($R = -1$) with frequency of 3 and 20 Hz. The extensometer base length was 12.5 mm.

Fig. 3 shows experimentally obtained data of S-N curve fitted using the Kohout-Věchet function [8]

$$\sigma = \sigma_\infty \cdot \left(\frac{N_f}{N_f + C} \right)^b \tag{1}$$

The regression led to the following values of parameters: $\sigma_\infty = 51.54$ MPa, $C = 314639$, $b = -0.1426$. The value of the sum of the squares of deviations $S = 74.73$ MPa^2 as well as Fig. 3 show that the fit of experimental data is quite satisfactory.

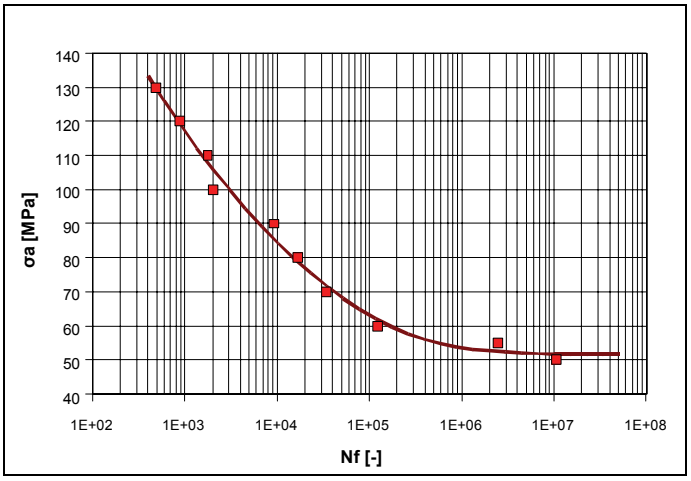

Fig. 3 Experimental data fitted using the Kohout-Věchet function.

The data presented in Fig. 3 can be also fitted using the Wöhler-Basquin equation [9]

$$\sigma_a = \sigma'_f \cdot (2N_f)^b \tag{2}$$

which is represented by straight line in log-log coordinates. The regression gives the values of material parameters $\sigma'_f = 216.89$ MPa, $b = -0.0969$.

Fig. 4 shows the derived Manson-Coffin curve: the experimentally obtained values of plastic deformation in $N_f/2$ cycles are fitted in log-log coordinates using power dependence (3) (the Manson-Coffin equation) [9]

$$\varepsilon_{ap} = \varepsilon'_f \cdot (2N_f)^c \tag{3}$$

The regression gives resulting values of fatigue parameters $\varepsilon'_f = 0.1455$, $c = -0.5891$.

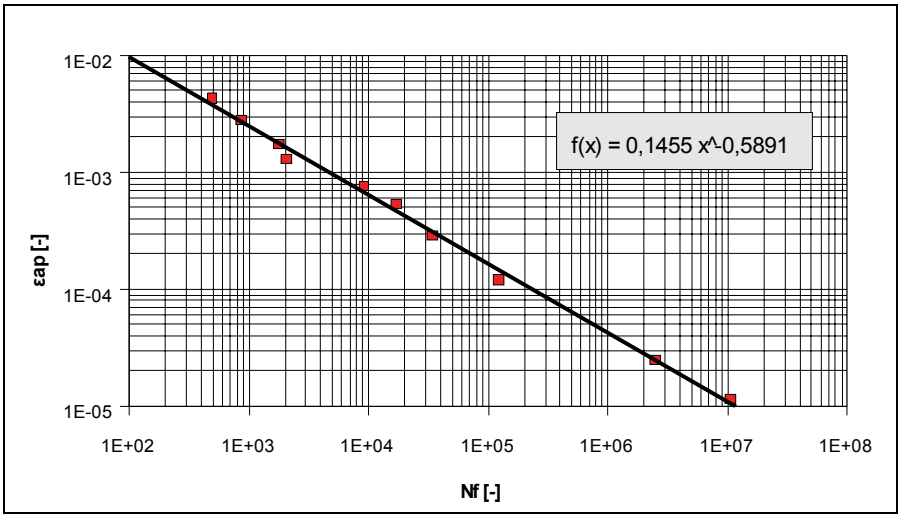

Fig. 4 The Manson-Coffin dependence.

The hysteresis loops for selected numbers of cycles to fracture are shown in Fig. 5. With growing number of cycles the loops become closed. Using analysis of hysteresis loops in $N_f/2$, the values of stress and strain were obtained which after fit with function (4) (modified Ramberg-Osgood equation) [10]

$$\varepsilon(\sigma) = \frac{\sigma}{E} + \left(\frac{\sigma}{\sigma_0}\right)^n \tag{4}$$

represent cyclic deformation curve described by the values of regression parameters $E = 46633.10$ MPa, $\sigma_0 = 462.31$ MPa, $n = 4.07$. Comparison of cyclic and tensile deformation curves (see Fig. 6) shows that the material becomes cyclically reinforced. This fact is also confirmed by the curves of cyclic hardening-softening where a decrease of plastic deformation up to one order can be seen at all stress amplitudes, see Fig. 7. The same figure also shows that there is no saturation during cyclic loading and the material reinforces cyclically during the whole fatigue life. This effect is more significant for lower stress amplitudes.

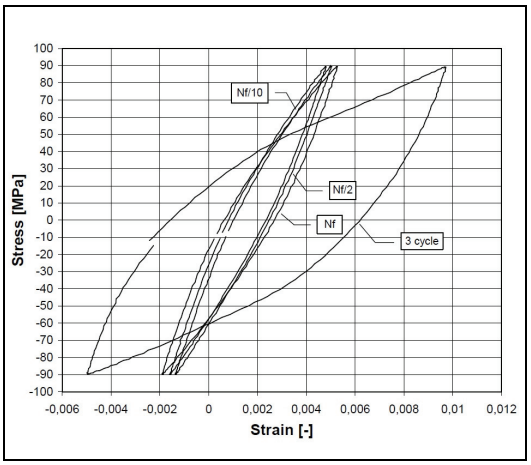

Fig. 5 Hysteresis loops for $\sigma_a = 90$ MPa.

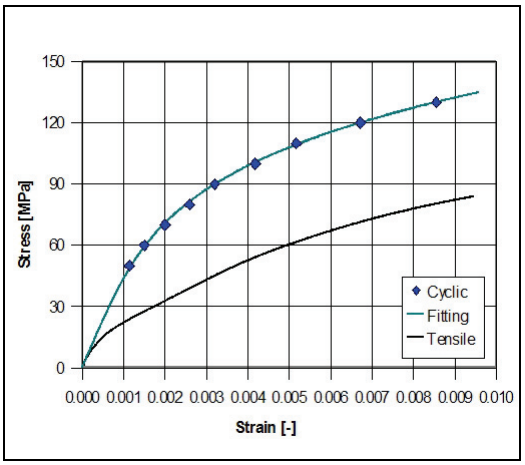

Fig. 6 Tensile and cyclic deformation curves.

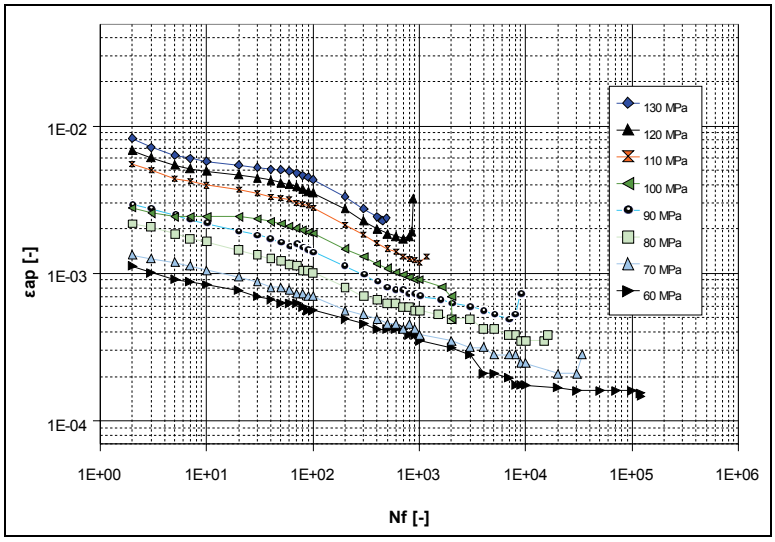

Fig. 7 Curves of cyclic hardening-softening.

Comparing the obtained results of fatigue behaviour determination with the results of e.g. [5] it can be said that the material reaches relatively good parameters with respect to the case of cast material.

3.4 Evaluation of fracture surfaces after fatigue loading

For documentation of fracture surfaces the Philips XL 30 scanning electron microscope has been used. Figs 8 and 9 show the fracture surfaces of test bars cyclically loaded at stress amplitude $\sigma_a = 60$ MPa. Fig. 8 shows the whole surface with marked place of crack initiation. The areas of crack growth and final rupture are easy to distinguish. The area of final rupture is created by transcrystalline ductile fracture while the area of fatigue crack growth is created by transcrystalline cleavage fracture. The detail view (Fig. 9) shows the initiation of fatigue crack.

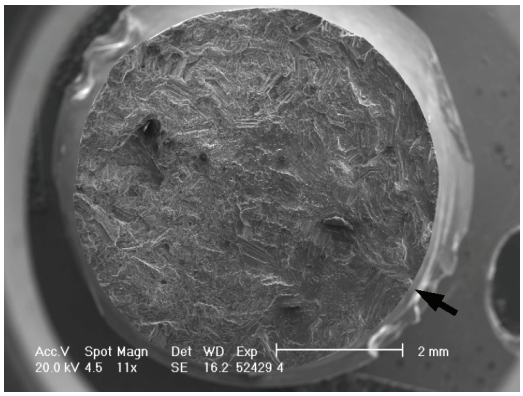

Fig. 8 Fracture surface, $\sigma_a = 60$ MPa, SEM.

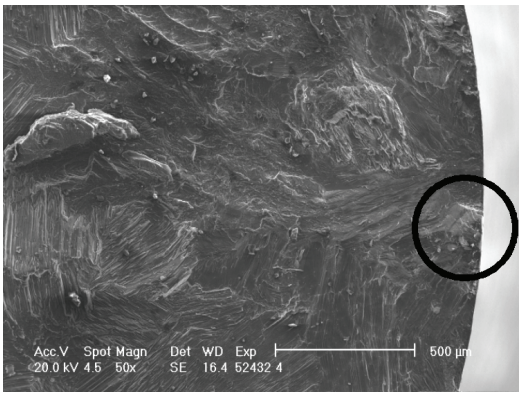

Fig. 9 Point of initiation, $\sigma_a = 60$ MPa, SEM.

Fracture surface of test bar cyclically loaded at stress amplitude $\sigma_a = 55$ MPa is shown in Fig. 10 where the places of crack initiation are marked. The areas of crack growth and final rupture are relatively easy to distinguish. Transcrystalline cleavage fracture is found in the area of crack growth while in the area of final rupture the transcristalline ductile fractureis observed. Fig. 11 shows the place crack growth area at higher magnification where the striations are clearly visible.

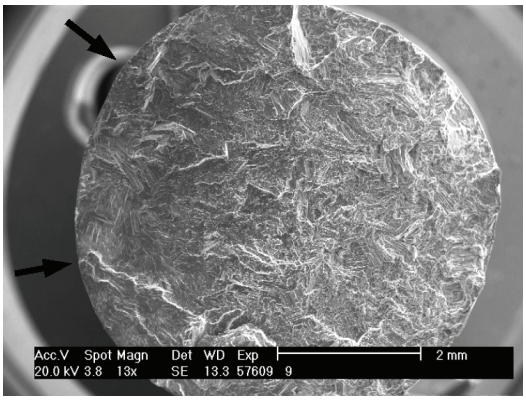

Fig. 10 Fracture surface, σ_a = 55 MPa, SEM.

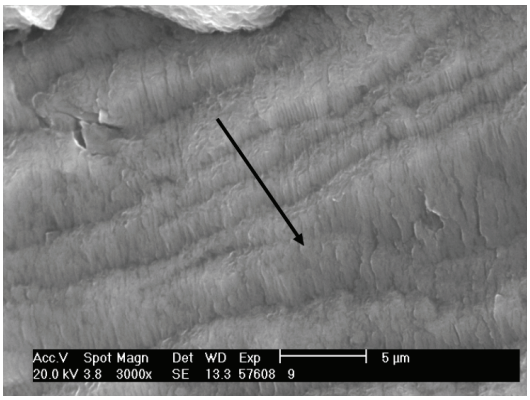

Fig. 11 Crack growth area, striations, marked direction of crack growth, σ_a = 55 MPa, SEM.

4 CONCLUSIONS

The chemical composition of investigated alloy corresponds to the usual composition according to the ASTM standard excluding the calcium added. The alloying elements including calcium mostly segregate to the grain boundaries. Manganese is the exclusion that forms variously distributed particles. The metallographic and local chemical analysis of the composition show that calcium in the structure of AZ 31 SC magnesium alloy occurs only on grain boundaries in the form of $(Mg, Al)_2Ca$ phase.

Static tensile tests determined the averages of tensile strength as R_m = 193 MPa and yield strength as $R_{p0,2}$ = 76 MPa. Also elongation to fracture A = 10.6 %, reduction of area Z = 9.7 %, and Young's modulus E = 40.9 GPa were assessed.

During fatigue tests two frequencies of loading cycle were used. Their change from 3 to 20 Hz did not cause any discontinuity in plotted experimental data.

The experimental results show that cyclic reinforcing is observed during the whole time of fatigue loading.

All fatigue tests were finished with fracture of test bars with exception of the tests with stress amplitude of 50 MPa, where the test bar was not broken and the test was stopped after reaching 10^7 cycles. The fatigue limit was determined for 10^8 cycles using regression as σ_C = 51.6 MPa.

The fatigue cracks initiate either on surface or on subsurface defects. The transcrystalline cleavage fracture is found in the area of fatigue crack growth and the transcrystalline ductile fracture in the area of final rupture.

Acknowledgments

Financial support of the Ministry of Education, Youth and Sports of the Czech Republic within the research project 1M2560471601 ***Eco-Centre for Applied Research of Non-Ferrous Metals*** **and within the development project No. 25/11** ***Reinforcing of students' motivation in master and postgraduate study programmes at Brno University of Technology*** **is gratefully acknowledged.**

REFERENCES

[1] PARK, J. P., KIM, M. G., YOON, U. S. & KIM, W. J. Microstructures and mechanical properties of Mg-Al-Zn-Ca alloys fabricated by high frequency electromagnetic casting method. *Journal of Materials Science*. 2009, 44. Nr. 1, Volume 44, pp. 47-54. ISSN 1573-4803.

[2] AVEDESIAN, M. M. & BAKER, H. *ASM Specialty Handbook: Magnesium and Magnesium Alloys*. Materials Park, OH : ASM International, 1999. ISBN 0-87170-657-1.

[3] DRÁPALA, J., KUCHAŘ, L., TOMÁŠEK, K., TROJANOVÁ, Z. *Hořčík, jeho slitiny a binární systémy hořčík-příměs.* Ostrava : Vysoká škola báňská – TU Ostrava, 2004. ISBN 80-248-0579-0.

[4] ALJARRAH, M., MEDRAJ, M., WANG, X., ESSADIQI, E., MUNTASAR, A. & DÉNÈS, G. Experimental investigation of the Mg–Al–Ca system. *Journal of Alloys and Compounds*. 2007, 436. Nr. 1-2, pp. 131-141. ISSN 0925-8388.

[5] HASEGAWA, S., TSUCHIDA, Y., YANO, H. & MATSUI, M. Evaluation of low cycle fatigue life in AZ31 magnesium alloy. *International Journal of Fatigue*. 2007, 29. Nr. 9-11, pp. 1839-1845. ISSN 0142-1123.

[6] CHAMOS, A. N., PANTELAKIS, Sp. G., HAIDEMENOPOULOS, G. N. & KAMOUTSI, E. Tensile and fatigue behaviour of wrought magnesium alloys AZ31 and AZ61. *Fatigue & Fracture of Engineering Materials & Structures*. 2008, 31. Nr. 9, pp. 812-821. ISSN 8756-758X.

[7] RUSZ, S. & ČÍŽEK, L.: Structure of Selected Magnesium Alloys Prepared for ECAP Application, *Hutnické listy*, č. 7, 2008, r. LXI, ISSN 0018-8069, p. 91 – 94.

[8] KOHOUT, J. & VĚCHET, S. A new function for description of fatigue curves and its multiple merits, *International Journal of Fatigue*. 2001, 23. No. 2, pp. 175-183. ISSN 0142-1123.

[9] KLESNIL, M. & LUKÁŠ, P. *Únava kovových materiálů při mechanickém namáhání.* Praha : Academia, 1975.

[10] ZAPLETAL, J., VĚCHET, S., KOHOUT, J. & LIŠKUTÍN, P. Fatigue lifetime of 7075 aluminium alloy from ultimate tensile strength to permanent fatigue limit. *Communications*. 2009, 11. Nr. 1, pp. 17-21. ISSN 1335-4205.